RJC

RASĀYAN *J. Chem.*
Vol. 18 | No. 2 |728-740| April - June | 2025
ISSN: 0974-1496 | e-ISSN: 0976-0083 | CODEN: RJCABP
http://www.rasayanjournal.com
http://www.rasayanjournal.co.in

METHYLENE BLUE DYE ADSORPTION ONTO MANILA TAMARIN SHELL COPPER NANOPARTICLES WITH RESPONSE SURFACE OPTIMIZATION

Dasari Kiran Kumar✉ and Pulipati King
Department of Chemical Engineering, AndhraUniversity College of Engineering, Andhra University, Visakhapatnam-530003, Andhra Pradesh, INDIA.
✉Corresponding author: dasarikirankumar018@gmail.com

ABSTRACT

In this study, Manila Tamarin Shell Copper nanoparticles (MTS-Cu-NPs) are used as a cheap adsorbent in batch research to get rid of the Methylene Blue dye in their water solution. Response surface methodology (RSM) is primarily concerned with the operational variables of initial concentration, adsorbent dose, solution pH, and temperature in a batch. The Central composite design (CCD) approach allows for the optimization of the process variables. Even when complex interactions are present, it is still used to determine the relative relevance of process elements. The highest possible removal efficiency was estimated by RSM with a value of 88.085% at the temperature of 309.07 K, a pH value of 4.79, the initial concentration of dye of 37.70 mg/L, an adsorbent dosage of 0.453 g/L, and adsorbent adsorption capability for Methylene blue dye removal is 88.22 mg/g.

Keywords: Adsorption, Methylene Blue Dye, Manila Tamarin Shell Copper Nanoparticles (MTS-Cu-Nps), Response Surface Methodology (RSM), Central Composite Design (CCD).

RASĀYAN *J. Chem.*, Vol. 18, No.2, 2025

INTRODUCTION

This review compares eco-friendly technologies for treating textile wastewater containing dye, highlighting their advantages and drawbacks, as they address the environmental and human health risks associated with dye pollution.[1] The study uses cashew nutshell as an inexpensive absorbent for Congo red dye removal from a solution of water. The best pH, dose, beginning dye concentration, time, and temperature were identified using the response surface central composite design approach.[2] The study assesses the adsorption capacity of cocoa bean shell powder as a bio adsorbent for Congo red dye, achieving maximum adsorption of 89.96% [3]. In the current study, investigators examine the removal of Congo red dye with Spathodea campanulata leaf powder as a low-cost biosorbent. Contact time, pH, starting dye concentration, biosorbent dosage, particle size, and temperature were among the parameters measured. The response surface methodology determines the ideal operational variables and their relevance.[4-5] The study investigates the adsorption capacity of methylene blue (MB) with activated carbon from coffee grounds (CAP). The three-factor Box-Behnken design optimizes the process, with pH, starting Methylene blue dye concentration, and CAP quantity all influencing adsorption. The best parameters for 91% degradation efficiency were identified as 0.05 g/L adsorbent weight, 100 mg/L dye concentration, and pH 2.5.[6] The study developed eco-friendly hydrogel beads from carboxymethyl cellulose, alginate, and graphene oxide using an ionotropic gelation technique. The biosorption process was optimized using a hybrid response surface methodology, with optimal conditions for Methylene blue removal.[7-9] The study utilized coconut husk cellulose as a cost-effective and eco-friendly adsorbent to remove methylene blue dye from aqueous solutions, optimizing the process with optimal parameters like initial Methylene blue dye concentration, contact time, and pH 7.[10-12] Research on fungal decolorization of dye wastewater explores mechanisms, elution and regeneration methods, pretreatment methods, and factors affecting decolorization.[13-17] Mordenite and nanocrystal effectively adsorb new methylene blue from aqueous solutions, with higher adsorption capacity. Adsorption kinetics follow pseudo-second-order kinetics, with higher pH resulting in higher adsorption capacity.[18-23]

EXPERIMENTAL

Preparing the Dye Solution

1 g of 100% Methylene Blue dye was added to 1000 mL of distilled water to create a stock solutions has a concentration of 1000 mg/L. The solution was produced in standard flasks. These stock solutions were then

http://doi.org/10.31788/RJC.2025.1829190

diluted to the desired dye concentration (10-100 mg/L) by mixing with a suitable proportion of distilled water.

Preparation of Manila Tamarind Shell Extract

Manila Tamarind Shell samples were washed with distilled water and ground into fine bits. Then, 20g of MTS powder was added with 100ml of double distilled water, well mixed, and cooked in a hot water bath for 45 minutes. The extract was then passed through Whatman No.41 filter paper, obtaining Manila Tamarind shell aqueous extract, which was refrigerated for later use.

General Procedure

Synthesis of Cu-NPs

4 g of copper sulfate pentahydrate and 100 cc of Manila Tamarind shell aqueous extract were magnetically swirled at room temperature (27 ^{o}C) for four hours. Within 10 minutes, the blue hue of copper sulfate pentahydrate turned brown, suggesting the creation of CuNPs as copper ions were reduced from Cu (II) ions to Cu metal. The samples were then centrifuged at 3000 rpm for 10 minutes to produce a clear, room-temperature supernatant. Copper nanoparticles were dried in an oven at 80-90 degrees Celsius for four hours before being analyzed using FT-IR, SEM, and XRD.[24-30]

Response Surface Methodology

The effective design and precise monitoring of adsorption technology are strongly dependent on the optimization of various process parameters based on dye removal. RSM is thus a precise and time-saving alternative to typical optimization approaches. The fundamental goal is to optimize the response surface, which is determined by process parameters. The effect of many process parameters on the removal of Methylene blue dye from aqueous solutions was explored using a complete factorial rotatable CCD (central composited design), including initial concentration (X1), biosorbent dosage (X2), solution pH (X3), and temperature (X4). A total of 29 trials were required, with 16 cube point runs, 8 axial point runs, 2 center point runs, 4 dummy runs, and duplicates of each experiment.

$$X_i = (X_i - X_{oi})/\Delta X_i \quad i= 1,2,3\ldots\ldots K \qquad (1)$$

Where Δxi is the step change, x_{0i} is the real value of the independent variable at the center point, x_i is the dimensionless value of an independent variable, and xi is its real value. Using STATISTICA 6.0 (Stat Soft Inc.), a second-degree polynomial equation (Eq. (2)) was created to estimate the percentage of dye adsorption at various biosorption process operating conditions.

$$Y = b_0 + b_1X_1 + b_2X_2 + b_3X_3 + b_4X_4 + b_{11}X_1 + b_{22}X^2_2 + b_{33}X^2_3 + b_{44}X^2_4 + b_{12}X_1X_2 + b_{13}X_1X_3 + b_{14}X_1X_4 + b_{23}X_2X_3 + b_{24}X_2X_4 + b_{34}X_3X_4 \qquad (2)$$

Where Y is the expected response, X_1, X_2, X_3, and X_4 are independent variables: b_0 is an offset term; b_1, b_2, b_3, and b_4 are linear effects; b_{11}, b_{22}, b_{33}, and b_{44} are squared effects and b_{12} , b_{13} , b_{14} , b_{23} , b_{24}, and b_{34} are interaction variables.

Table-1: Range of Parameters Covered

Parameters	Manila Tamarind Shell Copper Nanoparticles (MTS-CuNPs) adsorbent	
	Methylene blue	
	Min	Max
Contact time(t), min	5	100
Solution, pH	4	9
Adsorbent dosage, (w), (g/L)	0.1	0.8
Initial dye concentration, (C_0), (mg/L)	10	100
Temperature, (T), (K)	303	318

RESULT AND DISCUSSION

Effect of Contact Time

Figure-1 displays the percentage of adsorption that was measured at various contact times. According to the figure, the percentage of Methylene Blue dye removal grew sharply as contact time increased from 5 to 60 minutes. After reaching equilibrium for 60 minutes, the proportion of dye removal reached a plateau. Consequently, given the experimental setup employed in this investigation, 60 minutes of contact time is

adequate for the removal of Methylene Blue dye. For an initial dye concentration of 10 mg/L, the percentage of Methylene Blue dye removed using Manila Tamarind Shell Copper Nanoparticles (MTS-CuNPs) as an adsorbent increased from 60.49 to 92.01%, and the contact time increased from 5 to 100 minutes. With an increase in contact time from 5 to 60 minutes, the percentage of dye removal for 50 mg/L rose from 51 to 87.99% mg/g, respectively.

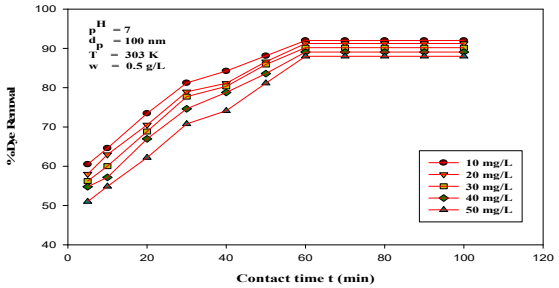

Fig.-1: Contact Time Effect on % Dye Removal of Methylene Blue Using Manila Tamarind Shell Copper Nanoparticles (MTS-CuNPs) as Adsorbent

Effect of Solution pH

One of the key regulating factors in the adsorption process is the pH of the solution. Using Fig.-2, the impact of solution pH on the percentage of dye removed for the removal of Methylene Blue dye was examined. At an initial concentration of 10 mg/L, the percentage of adsorption for Methylene Blue fell from 44 to 64% when the pH of the solution grew from 2 to 6, and also reduced as the pH of the solution increased from 6 to 9. When the solution's pH climbed from 2 to 9, the percentage of adsorption for Methylene Blue increased from 36% to 58% at an initial concentration of 50 mg/L. The maximum percentage of dye removal was discovered at pH 6.

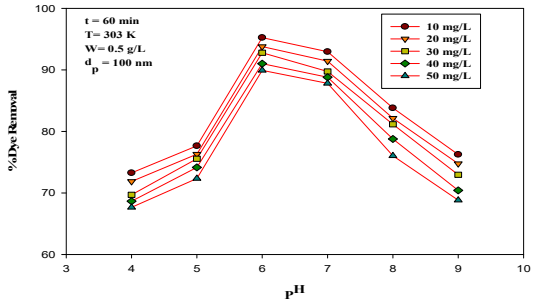

Fig.-2: Effect of Solution pH on % Dye Removal of Methylene blue Using Manila Tamarind Shell Copper Nanoparticles (MTS-CuNPs) as Adsorbent

Effect of Initial Concentration of Dye

Figure-3 illustrates how the initial dye concentration affects the percentage of dye removal. The figure clearly shows that when the original dye concentration increased from 10 to 100 mg/L, the percentage of dye removal declined. When the initial concentration of Methylene blue increased from 10 to 100 mg/L at 303 K, the percentage of dye removal of Methylene blue dropped from 94.80 to 88.16 percent.

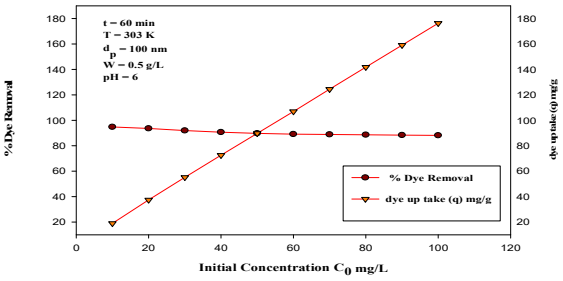

Fig.-3: Effect of Initial Concentration of Methylene blue on Dye Uptake and % Dye Removal using Manila Tamarind Shell Copper Nanoparticles (MTS-CuNPs Adsorbent

Effect of Biosorbent Dosage

The results, as shown in Fig.-4, show that increasing the adsorbent dosage enhanced the percentage of dye removal. At an initial concentration of 10 mg/L of Methylene blue, the percentage of dye removal rose from 61.04 to 94.44% when the adsorbent dosage was raised from 0.1 to 0.8 g/L. The percentage of dye removal rose from 50.25 to 89.36% for an initial concentration of Methylene blue of 50 mg/L when the adsorbent dosage was raised from 0.1 to 0.8. g/L.

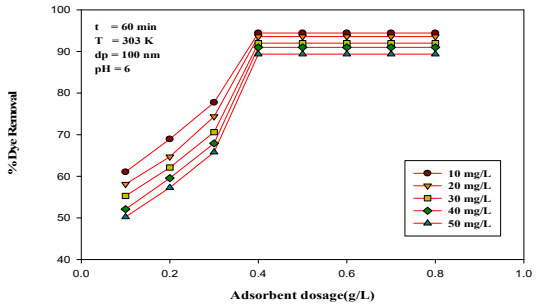

Fig.-4: Effect of Adsorbent Dosage on % Dye Removal of Methylene Blue Using Manila Tamarind Shell Copper Nanoparticles (MTS-CuNPs) as Adsorbent

Effect of Temperature

The outcome is displayed in Fig.-5. The graphic showed that as the solution's temperature rose, so did the percentage of dye elimination. This implies that the adsorption process is endothermic. When the solution temperature was raised from 303 K to 318 K, the percentage of dye removal increased from 94.26 to 96.37% and 89.78 to 92.13% for initial concentrations of Methylene Blue dye of 10 mg/L and 50 mg/L, respectively.

Optimization of Adsorption Process Variables with RSM

Temperature, solution pH, adsorbent dosage, and beginning concentration were all major factors in determining the percentage of dye adsorption by the adsorbent. To determine the perfect conditions for the highest percentage of methylene blue dye adsorption onto MTS-Cu-NPs adsorbent using RSM, these four factors were chosen as independent variables. Using full factorial CCD (Central composite design), the effects of several process variables, including initial dye concentration (X_1), biosorbent dosage (X_2) solution pH (X_3), and temperature (X_1), on the adsorption of Methylene blue onto the adsorbent were investigated. The proportion of Methylene Blue dye adsorption was used to express the reaction. Methylene blue dye was removed from the aqueous solution by optimizing process variables using a CCD across 29 experiments, which included 16 cube point runs, 8 center point runs, 2 axial point runs, and 4 dummy runs. Eq. (4) was utilized to code all independent variables for statistical analysis. The range of variables used in this design was selected and tabulated in Table-2, and the experimental design matrix, as well as the percentage of Methylene blue adsorption, in Table-3, based on preliminary experimental data.

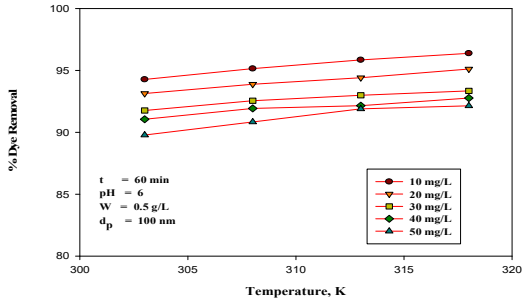

Fig.-5: Effect of Temperature on % Dye Removal of Methylene Blue using Manila Tamarind Shell Copper Nanoparticles (MTS-CuNPs) as Adsorbent

Development of Regression Model Equation

The Central Composited design-response surface methodology was used to develop a correlation model between MB adsorption capacity and preparation parameters, with a center point of 5 per block. Tables-4, 5, and 6 contain the sum of squares, lack of fit tests, and model summary statistics, which provide an overview of the sequential model's parameters. According to the data, a quadratic model for Methylene blue

adsorption on MTS-Cu-NPs is suggested. Regression analysis was also employed to fit the MB adsorption response function to MTS-Cu-NPs. The preferred quadratic model for calculating MB adsorption is Eq. (4), which shows the Methylene blue adsorption (qe) as a function of Initial Concentration (A, mg/L), Adsorbent Dosage (B, g/L), Solution pH (C), and Temperature (D, K). The variables in this model have coded values (-2, -1, 0, 1, 2).

Table-2: Levels of Different Process Variables Used in CCD for the Adsorption of Methylene Blue Dye onto Manila Tamarin Shell Copper Nanoparticles (MTS-Cu-Nps) Adsorbent

Variable	Name	Range and Levels				
		-2	-1	0	1	2
X1	Initial dye Concentration, C_0, mg/L	10	20	30	40	50
X2	Adsorbent Dosage, w, g/L	0.3	0.4	0.5	0.6	0.7
X3	pH of Solution	4	5	6	7	8
X4	Temperature, T K	298	303	308	313	318

Coded Factors of Final Equation

$$\text{Dye Removal \%} = 92.61 - 0.4756\,A + 1.01\,B + 1.08\,C + 2.67\,D + 0.0988\,AB - 0.1112\,AC + 0.1188\,AD - 0.4237\,BC + 0.1313\,BD + 0.3063\,CD - 1.3\,A^2 - 3.79\,B^2 - 8.89\,C^2 - 1.99\,D^2 \quad (3)$$

The equation in terms of coded factors can be used to anticipate the response for specific levels of each factor. By default, the highest values of the components are coded as +2, while low levels are written as -2. The coded equation is useful for determining the relative impact of the elements by comparing their coefficients.

Table-3: Shows the Experimental Design Matrix and the Percentage of Methylene Blue Dye Adsorption onto the Manila Tamarin Shell Copper Nanoparticles (MTS-Cu-NPs) Adsorbent

Experimental Run	X_1	X_2	X_3	X_4	% Adsorption of Methylene blue	
					Experiment	Predicted
15	-2	-2	-2	-2	72.11	72.49
13	2	-2	-2	-2	71.04	71.32
10	-2	1	-2	-2	74.44	74.89
2	2	1	-2	-2	73.73	74.12
12	-2	-2	2	-2	74.74	75.11
29	2	-2	2	-2	73.02	73.5
4	-2	1	2	-2	75.54	75.82
24	2	1	2	-2	75.02	74.6
3	-2	-2	-2	2	76.47	76.71
5	2	-2	-2	2	76.11	76.02
6	-2	1	-2	2	79.93	79.64
19	2	1	-2	2	79.89	79.35
20	-2	-2	2	2	80.76	80.56
8	2	-2	2	2	80.05	79.43
28	-2	1	2	2	82.25	81.8
17	2	1	2	2	81.24	81.06
7	-2	0	0	0	92.56	91.79
21	2	0	0	0	90.14	90.84
22	0	-2	0	0	88.67	87.81
23	0	1	0	0	89.05	89.83
25	0	0	-2	0	83.45	82.64
18	0	0	2	0	84.07	84.81
26	0	0	0	-2	90.16	87.95

11	0	0	0	2	91.16	93.29
27	0	0	0	0	92.56	92.61
16	0	0	0	0	92.56	92.61
1	0	0	0	0	92.56	92.61
9	0	0	0	0	92.56	92.61
14	0	0	0	0	92.56	92.61

Actual Factors of Final Equation

$$\text{dye Removal \%} = -1945.14322 - 0.007833\,A + 85.09908\,B + 23.09861\,C + 12.36137\,D + 0.024687\,AB - 0.002781\,AC + 0.000594\,AD - 1.05938\,BC + 0.065625\,BD + 0.015312\,CD - 0.003241\,A^2 - 94.66262\,B^2 - 2.22163\,C^2 - 0.019865\,D^2 \quad \text{Eq. (4)}$$

The equation in terms of actual variables can be employed to predict the reaction for certain levels of each factor. The levels for every variable should be provided in their original units. This equation should not be used to calculate the relative impact of each element since the coefficients have been scaled to suit the units of each factor, and the intercept is not in the center of the design space. Positive signals show synergistic effects, whereas negative signs show antagonistic actions.

Table-4: Sum of Squares

Source	Sum of Squares	df	Mean Square	F-value	p-value	
Mean vs Total	1.98E+05	1	1.98E+05			
Linear vs Mean	171.8	4	42.95	0.7121	0.5917	
2FI vs Linear	5.23	6	0.8715	0.0109	1	
Quadratic vs 2FI	1426.95	4	356.74	325.24	< 0.0001	Suggested
Cubic vs Quadratic	15.2	8	1.9	72.55	< 0.0001	Aliased
Residual	0.1571	6	0.0262			
Total	2.00E+05	29	6895.7			

Choose the highest-order polynomial whose additional terms are significant, and the model is not aliased.

Statistical Analysis

Table-6 shows an evaluation of the developed quadratic model's quality based on the correlation coefficient. The predicted R-squared assesses how well the model predicts response data, whereas the adjusted R-squared indicates how much volatility around the mean is explained by the quadratic model. The R-squared, adjusted R-squared, and predicted R-squared for Eq. (2) are 0.9905, 0.981, and 0.9567, respectively, as shown in Table-6. The difference between the adjusted R-squared of 0.981 and the expected R-squared of 0.9567 is less than 0.2, indicating reasonable agreement. Furthermore, the regression model's standard deviation (SD) is 1.05. As a result, the experimental and anticipated values are very similar. The analysis of variance (ANOVA) further verified the regression model's relevance and applicability. Furthermore, Table-7 displays the findings, which show that the quadratic model has a significant impact on The Model F-value of 104.46 indicates that the model is significant. There is just a 0.01% chance that an F-value this large will occur owing to noise. P-values of less than 0.0500 suggest that model terms are significant. In this scenario, B, C, D, B^2, C^2, and D^2 are important model terms. Values above 0.1000 imply that the model terms are not significant. If your model has a large number of irrelevant terms (not including those required to support hierarchy), model reduction may improve it. Figure-6 shows a comparison of the actual and expected values for MB adsorption capabilities. It is clear that the anticipated results closely match the experimental values, indicating that the regression model developed is successfully exposing the relationship between the MB's ability to absorb and preparatory parameters. Figures-8 and 9 show the quadratic model's residual vs expected and residual versus Run graphs. The mean value of the residuals is

normal, as indicated by Fig.-7, which shows that the residuals' normal probability distribution is approximately linear. Furthermore, the data residuals have an unequal distribution.

Table-5: Lack of Fit Tests

Source	Sum of Squares	df	Mean Square	F-value	p-value
Linear	1447.53	20	72.38		
2FI	1442.3	14	103.02		
Quadratic	15.36	10	1.54		
Cubic	0.1571	2	0.0786		
Pure Error	0	4	0		

The selected model should have an insignificant lack of fit.

Table-6: Model Summary Statistics

Source	Std. Dev.	R^2	Adjusted R^2	Predicted R^2	PRESS	
Linear	7.77	0.1061	-0.0429	-0.2602	2040.71	
2FI	8.95	0.1093	-0.3855	-2.2787	5309.36	
Quadratic	1.05	0.9905	0.981	0.9567	70.09	Suggested
Cubic	0.1618	0.9999	0.9995	0.9777	36.09	Aliased

Prioritize the model that maximizes both the adjusted and predicted R^2.

Table-7: ANOVA for the Quadratic Model for Removing Methylene Blue Dye

Source	Sum of Squares	df	Mean Square	F-value	p-value	
Model	1603.98	14	114.57	104.46	< 0.0001	significant
A-IC	4.07	1	4.07	3.71	0.0746	
B-Dosage	18.24	1	18.24	16.63	0.0011	
C-pH	21.17	1	21.17	19.3	0.0006	
D-Temp	128.32	1	128.32	116.99	< 0.0001	
AB	0.156	1	0.156	0.1423	0.7117	
AC	0.198	1	0.198	0.1805	0.6774	
AD	0.2256	1	0.2256	0.2057	0.6571	
BC	2.87	1	2.87	2.62	0.1279	
BD	0.2756	1	0.2756	0.2513	0.624	
CD	1.5	1	1.5	1.37	0.2617	
A^2	4.35	1	4.35	3.96	0.0664	
B^2	37.07	1	37.07	33.8	< 0.0001	
C^2	204.2	1	204.2	186.17	< 0.0001	
D^2	10.2	1	10.2	9.3	0.0086	
Residual	15.36	14	1.1			
Lack of Fit	15.36	10	1.54			
Pure Error	0	4	0			
Cor Total	1619.33	28				

The coefficient estimate shows the expected change in response per unit change in factor value when all other factors stay constant. In an orthogonal design, the intercept represents the overall average response of all runs. The coefficients alter the average based on the factor settings. When the factors are orthogonal, the VIFs are 1. VIFs greater than 1 imply multi-colinearity the higher the VIF, the more severe the factor correlation. VIFs under 10 are generally acceptable.

Response Surface Methodology Plots

The greatest F-value of 104.46, as indicated in Table-7, suggests that all pretreatment parameters had a greater impact on MB adsorption capacity.

Table-8: The Response of the Surface Coefficients of Regression for the Removal of Methylene Blue Dye in Terms of Coded Variables

Factor	Coefficient Estimate	df	Standard Error	95% CI Low	95% CI High	VIF
Intercept	92.61	1	0.3423	91.87	93.34	
A-IC	-0.4756	1	0.2469	-1	0.0539	1
B-Dosage	1.01	1	0.2469	0.4772	1.54	1
C-pH	1.08	1	0.2469	0.555	1.61	1
D-Temp	2.67	1	0.2469	2.14	3.2	1
AB	0.0988	1	0.2618	-0.4628	0.6603	1
AC	-0.1112	1	0.2618	-0.6728	0.4503	1
AD	0.1188	1	0.2618	-0.4428	0.6803	1
BC	-0.4237	1	0.2618	-0.9853	0.1378	1
BD	0.1313	1	0.2618	-0.4303	0.6928	1
CD	0.3063	1	0.2618	-0.2553	0.8678	1
A^2	-1.3	1	0.6513	-2.69	0.1004	2.64
B^2	-3.79	1	0.6513	-5.18	-2.39	2.64
C^2	-8.89	1	0.6513	-10.28	-7.49	2.64
D^2	-1.99	1	0.6513	-3.38	-0.5896	2.64

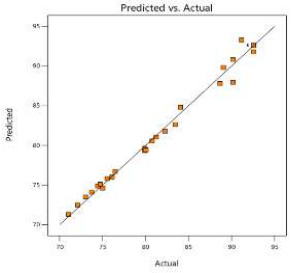

Fig.-6: Dye Removal % of Predicted vs Actual

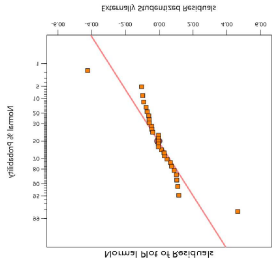

Fig.-7: Normal plot of Residuals

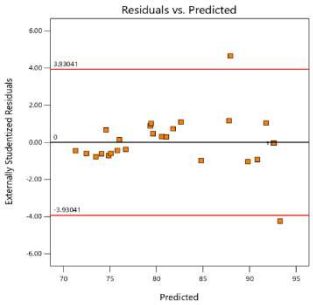

Fig.-8: Residuals vs Predicted

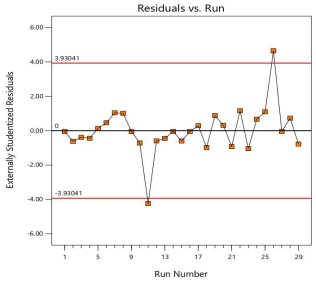

Fig.-9: Residuals vs Run

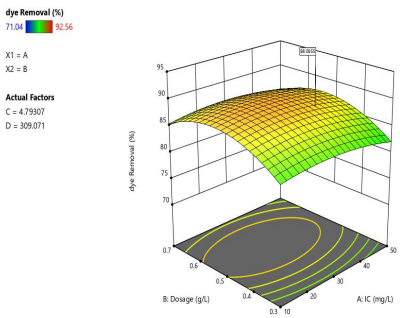

Fig.-10: A 3D Response Surface Plot of Initial Dye Concentration Against Absorbent Dosage for Methylene Blue Adsorption

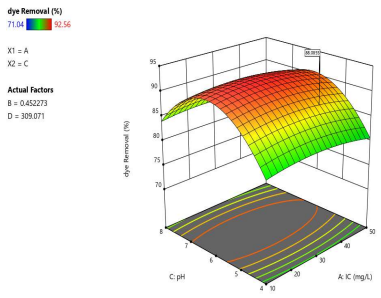

Fig.-11: A 3D Response Surface Plot of Initial Dye Concentration against pH for Methylene Blue Adsorption

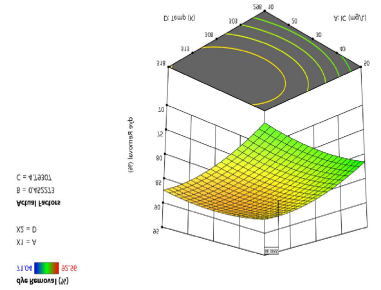

Fig.-12: A 3D Response Surface Plot of Initial Dye Concentration against Temperature for Methylene Blue Adsorption

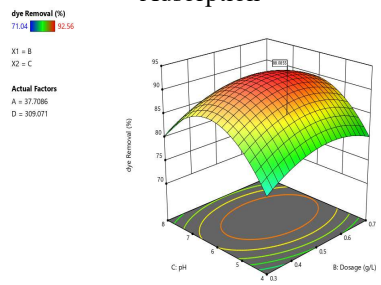

Fig.-13: A 3D Response Surface Plot of Absorbent Dosage against pH for Methylene Blue Adsorption

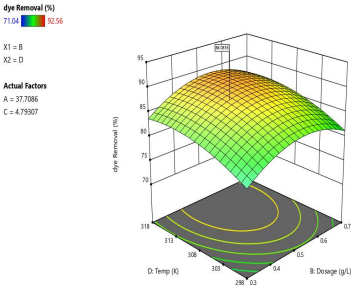

Fig.-14: A 3D Response Surface Plot of Absorbent Dosage Against Temperature for Methylene Blue Adsorption

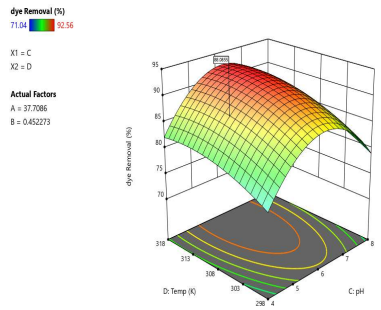

Fig.-15: A 3D Response Surface Plot of pH against Temperature for Methylene Blue Adsorption

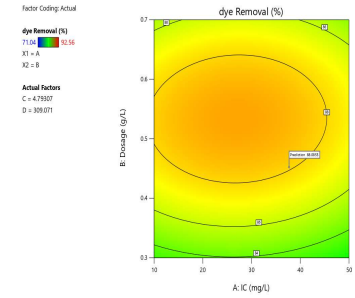

Fig.-16: A Contour Plot of the Response Surface of Initial Concentration Against Adsorbent Dosage for Methylene Blue Adsorption

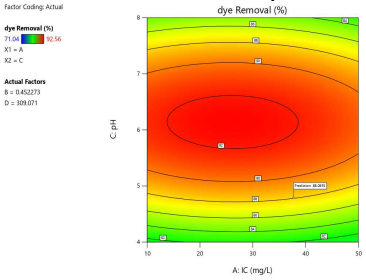

Fig.-17: A Contour Plots of Response Surface of pH against Initial Concentration for Methylene Blue Adsorption

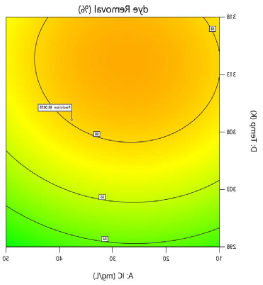

Fig.-18: A Contour Plots of Response Surface of Initial Concentration against Temperature for Methylene Blue Adsorption

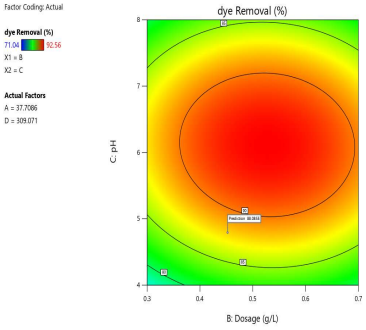

Fig.-19: A Contour Plots of Response Surface of pH against Adsorbent Dosage for Methylene Blue Adsorption

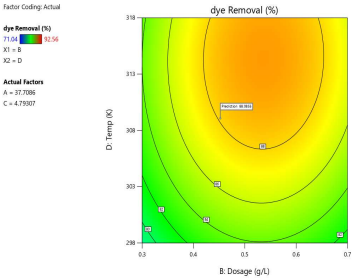

Fig.-20: A Contour Plots of Response Surface of Adsorbent Dosage Against Temperature for Methylene Blue Adsorption

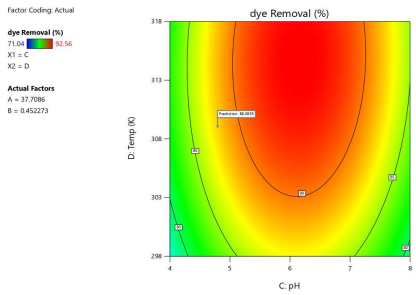

Fig.-21: A Contour Plots of Response Surface of pH against Temperature for Methylene Blue Adsorption

Furthermore, the correlations between Initial Concentration and Temperature (AD), Adsorbent dosage and Solution pH (BC), and Adsorbent dosage and Temperature (BD) had a significant effect on MB adsorption capacity, as opposed to Initial Concentration and Adsorbent dosage (AB), Initial Concentration and Solution pH (AC), and Solution pH and Temperature (CD) (the F-values of AD, BC, and BD are 0.1423, 0.1805, 0.2057, 2.62, 0.2513, and 1.37, respectively). Figures 10 to 15 indicate that the relationship between variables becomes increasingly apparent as the contour approaches the ellipse. With a pH of 4.79 and a temperature of 309.07 K, Fig. 10 shows the combined effect of the starting concentration and adsorbent dosage on Methylene blue adsorption capacity. Figure-16 depicts the findings, which show that the interaction becomes increasingly visible as the contour approaches the ellipse. With an adsorbent dosage of 0.453 g/L and a temperature of 309.07 K, Fig.-11 shows the combined effect of initial concentration and pH solution on Methylene blue adsorption capacity. Figure-17 shows that the Methylene blue adsorption capacity initially increases and subsequently decreases as the initial concentration increases, indicating that the Methylene blue adsorption capacity decreases at lower starting concentrations. With an adsorbent dose of 0.453 g/L and a pH of 4.79, Fig.-12 shows how starting concentration and temperature affect Methylene blue adsorption capacity. The results are also given in Fig.-18, which show that the interaction becomes increasingly visible as the contour approaches the ellipse. With an initial concentration of 37.70 mg/L and a temperature of 309.07, Fig.-13 shows the combined effect of adsorbent dose and pH on Methylene blue adsorption capacity. The findings are also displayed in Fig.-19, which shows that the interaction becomes increasingly visible as the contour approaches the ellipse. Figure-14 depicts the combined impact of absorbent dosage and temperature on MB adsorption capacity at an initial concentration of 37.70 mg/L and a pH of 4.79. Figures-20 illustrates the findings as well. With an initial concentration of 37.70 mg/L and an adsorbent dosage of 0.453 g/L, Fig. 15 shows the combined effect of pH and temperature on MB adsorption capacity. Figure-21 illustrates the findings as well.

Optimization

RSM optimization techniques were utilized to optimize the preparation parameters to determine the maximal Methylene blue adsorption capability. The initial concentration of 37.70 mg/L, adsorbent dosage of 0.453 g/L, pH of 4.79, and Temperature of 309.07 K were determined to be the ideal preparation parameters following the computation. Furthermore, the quadratic model predicts that MTS-Cu-NPs produced under optimal preparation conditions will have an MB adsorption capacity of adsorbent for the elimination of Methylene blue dye of 88.22 mg/g, with a desirability of approximately 1.

CONCLUSION

Adsorption tests revealed that a contact period of 60 minutes was adequate to remove the greatest amount of Methylene blue dye from aqueous solution using the Manila Tamarin shell Copper Nanoparticles (MTS-Cu-NPs) adsorbent. The highest removal efficiency was estimated by RSM to be 88.085% at a temperature of 309.07 K, solution pH of 4.79, initial dye concentration of 37.70 mg/L, adsorbent dosage of 0.453 g/L, and adsorbent adsorption ability for Methylene blue dye removal is 88.22 mg/g.

ACKNOWLEDGEMENTS

I express my sincere gratitude to B.V. Raju Institute of Technology for providing access to their well-equipped laboratory facilities, enabling the successful execution of experiments crucial to this research paper.

CONFLICT OF INTERESTS

There is no conflict of interest, according to the authors.

AUTHOR CONTRIBUTIONS

All the authors contributed significantly to this manuscript, participated in reviewing/editing and approved the final draft for publication. The research profile of the authors can be verified from their ORCID ids, given below:

Dasari Kiran Kumar https://orcid.org/0000-0002-8719-7613
Pulipati King https://orcid.org/0000-0001-8210-3019

REFERENCES

1. S. A. Akintelu, A. K. Oyebamiji, S. C. Olugbeko, and D. F. Latona, *Current Research in Green and Sustainable Chemistry*, **4,** 100176(2021), https://doi.org/10.1016/j.crgsc.2021.100176
2. A. H. Jawad, A. S. Abdulhameed, T. Khadiran, Z. A. ALOthman, L. D. Wilson, and S. Algburi, *International Journal of Phytoremediation*, **26(5),** 727(2024), https://doi.org/10.1080/15226514.2023.2262040
3. D. Allouss, Y. Essamlali, O. Amadine, A. Chakir, and M. Zahouily, *RSC Advances*, **9(65)**, 37858(2019), https://doi.org/10.1039/c9ra06450h
4. R. A. Tohamy, S. S. Ali, F. Li, K. M. Okasha, Y. A. G. Mahmoud, T. Elsamahy, H. Jiao, Y. Fu, and, J. Sun, *Ecotoxicology and Environmental Safety,* **231,** 113160(2022), https://doi.org/10.1016/j.ecoenv.2021.113160
5. D. Mansour, E. Alblawi, A.K.D. Alsukaibi, and B. A. Shammari, *Sustainable Water Resource Management,* **10**, 41(2024), https://doi.org/10.1007/s40899-023-01022-x
6. D. Azzouni, F. Baragh, A. M. Mahmoud, M. M. Alanazi, Z. Rais, and M. Taleb, *Journal of Saudi Chemical Society*, **27(5),** 101695 (2023), https://doi.org/10.1016/j.jscs.2023.101695
7. L. Brahmi, F. Kaouah, S. Boumaza, and M. Trari, *Applied Water Science*, **9(8),** 1(2019), https://doi.org/10.1007/s13201-019-1053-2
8. S. Daikh, D. Ouis, A. Benyoucef, and B. Mouffok, *Chemical Physics Letters*, **798,** 139565(2022), https://doi.org/10.1016/j.cplett.2022.139565
9. S. Dawood and T. K. Sen, *Water Research*, **46(6),** 1933(2012), https://doi.org/10.1016/j.watres.2012.01.009
10. D. Dimbo, M. Abewaa, E. Adino, A. Mengistu, T. Takele, A. Oro, and M. Rangaraju, *Results in Engineering*, **21,** 101910(2024), https://doi.org/10.1016/j.rineng.2024.101910
11. Y. Fu, and T. Viraraghavan, *Bioresource Technology*, **79(3),** 251(2001), https://doi.org/10.1016/S0960-8524(01)00028-1
12. V. V. Gedam, P. Raut, A. Chahande, and P. Pathak, *Applied Water Science*, **9(3),** 55(2019), https://doi.org/10.1007/s13201-019-0933-9
13. M. K. Ghosh, S. Sahu, I. Gupta, and T. K. Ghorai, *RSC Advances*, **10(37)**, 22027(2020), https://doi.org/10.1039/d0ra03186k
14. A. Jabeen, and H. N. Bhatti, *Environmental Technology and Innovation*, **23**, 101685(2021), https://doi.org/10.1016/j.eti.2021.101685
15. R. Kabbout, and S. Taha, *Physics Procedia*, **55,** 437(2014), https://doi.org/10.1016/j.phpro.2014.07.063
16. D. Kavitha, and C. Namasivayam, *Bioresource Technology*, **98(1),** 14(2007), https://doi.org/10.1016/j.biortech.2005.12.008
17. M. Khosravi, and S. Arabi, *Water Science and Technology: A Journal of the International Association on Water Pollution Research*, **74(2),** 343(2016), https://doi.org/10.2166/wst.2016.122
18. I. Loulidi, F. Boukhlifi, M. Ouchabi, A. Amar, M. Jabri, A. Kali, and F. Aziz, *Physical Chemistry Research*, **8(3),** 569(2020), https://doi.org/10.22036/pcr.2020.225170.1751

19. I. D. Mall, V. C. Srivastava, N. K. Agarwal, and I. M. Mishra, *Chemosphere*, **61(4),** 492(2005), https://doi.org/10.1016/J.Chemosphere.2005.03.065
20. D. A. Naidu, N. Saibaba, P. King, and V. S. R. K. Prasad, *International Journal of Research in Engineering and Technology,* **1(2)**, 35(2013)
21. K. S. Obayomi, S. Y. Lau, M. K. Danquah, J. Zhang, T. Chiong, O. V. Obayomi, L. Meunier, and M. M. Rahman, *Process Safety and Environmental Protection*, **184,** 129(2024), https://doi.org/10.1016/j.psep.2024.01.106
22. F. O. Omwoyo, and G. Otieno, *Journal of Materials Science and Chemical Engineering*, **12(02),** 1(2024), https://doi.org/10.4236/msce.2024.122001
23. S. Ponnusamy, and R. Subramaniam, *International Journal of Industrial Chemistry*, **4(1),** 17(2013), https://doi.org/10.1186/2228-5547-4-17
24. M. Rahmani, B. Regraguy, J. Mabrouki, A. Moufti, M. El'mrabe, A. Dahchour, and S. E. Hajjaji, *Desalination and Water Treatment*, **244,** 253(2021), https://doi.org/10.5004/dwt.2021.27897
25. K. R. Ramakrishna, and T. Viraraghavan, *Water Science and Technology*, **36(2–3),** 189(1997), https://doi.org/10.2166/wst.1997.0516
26. M. Ravikumar, and P. King, *Rasayan Journal of Chemistry*, **12(4),** 2318(2019), https://doi.org/10.31788/RJC.2019.1244034
27. G. R. Arellano, J. B. Fernández, R., G. Alamilla, L. M. L. Galvez, A. H. L. Rivera, and P. G. Alamilla, *Materials*, **14(11**), 2763(2021), https://doi.org/10.3390/ma14112763
28. A. Saravanan, S. Karishma, P. S. Kumar, S. Varjani, P. R. Yaashikaa, S. Jeevanantham, R. Ramamurthy, and B. Reshma, *Chemosphere*, **271,** 129519(2021), https://doi.org/10.1016/j.chemosphere.2020.129519
29. S. A. Umoren, U. J. Etim, and A. U. Israel, *Journal of Material and Environmental Science*, **4(1),** 75(2013)
30. P. Waranusantigul, P. Pokethitiyook, M. Kruatrachue, and E. S. Upatham, *Environmental Pollution*, **125(3),** 385(2003), https://doi.org/10.1016/S0269-7491(03)00107-6

[RJC-9190/2024]